Membrane binding and oligomer formation by the calcium-dependent lipopeptide antibiotic A54145: a quantitative study with pyrene excimer fluorescence

TianHua Zhang, Scott D. Taylor, Michael Palmer*, Jean Duhamel*

Department of Chemistry, University of Waterloo, Waterloo, ON N2L 3G1, Canada

Abstract

A54145 is a lipopeptide antibiotic related to daptomycin that permeabilizes bacterial cell membranes. Its action requires both calcium and phosphatidylglycerol in the target membrane, and it is accompanied by the formation of membrane-associated oligomers. We here probed the interaction of A54145 with model membranes composed of dimyristoyl-phosphatidylcholine and dimyristoyl-phosphatidylglycerol, using the steady-state and time-resolved fluorescence of a pyrene-labelled derivative (Py-A54145). In solution, the labelled peptide was found to exist as a monomer. Its membrane interaction occurred in two stages that could be clearly distinguished by varying the calcium concentration. In the first stage, which was observed between 0.15 and 1 mM calcium, Py-A54145 bound to the membrane, as indicated by a strong increase in pyrene monomer emission. At the same time calcium concentration, excimer emission increased also, which suggested oligomerization of Py-A54145. A global analysis of the time-resolved pyrene monomer and excimer fluorescence confirmed that Py-A54145 forms oligomers quantitatively and concomitantly with membrane binding. When calcium was raised beyond 1 mM, a distinct second transition was observed that may correspond to a doubling of the number of oligomer subunits. The collective findings confirm and extend our understanding of the action mode of A54145 and daptomycin.

Keywords: calcium-dependent lipopeptide antibiotics, phosphatidylglycerol, pyrene fluorescence, time-resolved fluorescence

*Corresponding authors

Email addresses: oscarzhang@hotmail.com (TianHua Zhang), s5taylor@uwaterloo.ca (Scott D. Taylor), mpalmer@uwaterloo.ca (Michael Palmer), jduhamel@uwaterloo.ca (Jean Duhamel)

1. Introduction

The lipopeptide antibiotic A54145 [1] is homologous to daptomycin, a clinically important drug that is used in the treatment of infections with Gram-positive bacteria [2]. Both antibiotics bind to the bacterial cell membrane and cause its depolarization [3, 4], and with both molecules, this involves the formation of membrane-associated oligomers. Mixtures of both antibiotics even give rise to hybrid, partially functional oligomers [5], which suggests a closely similar mode of action. The two compounds differ, however, in two criteria that are important for clinical application. A54145 is too toxic for application in humans; on the other hand, it is not inhibited by lung surfactant. Daptomycin, which is much less toxic, is strongly inhibited by surfactant, which limits its usefulness for treating pneumonia [6]. The creation of hybrid derivatives that combine the useful traits of both has been attempted [7].

While the interaction of daptomycin with cell membranes is not yet fully understood, it is known that specific lipids have important roles in membrane susceptibility and resistance. In model liposomes, phosphatidylglycerol (PG) was found to be essential for oligomer formation and membrane permeabilization [8, 9], and in bacteria, increased conversion of PG to lysyl-PG correlates with resistance to daptomycin [10]. The evidence on a role of cardiolipin in bacterial daptomycin resistance is ambiguous [11, 12], but it is noteworthy that cardiolipin can inhibit membrane permeabilization in a liposome model [13].

In a recent study, we explored the ternary interaction of daptomycin and A54145 with PG and calcium using isothermal calorimetry and fluorescence [14]. When Ca^{2+} concentrations were raised successively from 0 to 1 mM and beyond, two successive calcium-dependent transitions were observed, which correspond to the binding of two Ca^{2+} ions to each lipopeptide molecule. Fluorescence results indicated that both peptides bound to the membrane concomitantly with binding of the first Ca^{2+} ion, whereas oligomer formation was apparent only when the second ion had bound also. It must be noted, however, that all the fluorescent probes used in that study were part of or attached to the peptide moiety (cf. Figure 1), whereas the behaviour of the fatty acyl tail was not observed.

With daptomycin, the behaviour of the fatty acyl tail had been studied earlier by incorporating a perylene moiety into it [15]. Perylene molecules in close proximity will form excited dimers (excimers), and the labelled lipopeptide indeed produced a strong excimer signal upon oligomerization, indicating that the acyl residues are in close proximity within the oligomer.

A more established fluorescence probe of molecular proximity is pyrene [16]. Compared to perylene, pyrene excimers display stronger fluorescence

that also is spectrally better separated from that of the monomer. Daptomycin contains a kynurenine residue, which interferes with pyrene fluorescence [15]. However, A54145 does not contain a kynurenine residue, and we here used pyrene fluorescence to probe the membrane interaction of this lipopeptide.

Pyrene forms excimers when two molecules come within 10 Å of each other [17]. Moreover, the fluorescence intensity and lifetime of the pyrene monomer undergo a large increase upon translocation from water to an apolar and highly viscous environment, such as the interior of lipid bilayers [18–24]. This combination of traits makes pyrene a versatile and informative probe not only of proximity but also of environmental change. In the context of protein structure and function, pyrene has been widely used to study interactions with lipid bilayers, substrates, ions, or denaturants, as well as inter- and intramolecular spatial relationships (see for example references 16, 22, and 24).

Without exception, all previous biophysical applications of pyrene have relied on the analysis of the steady-state fluorescence, while the fluorescence decays of the pyrene-labelled molecules were deemed too complex and never quantitatively analysed. In contrast to these earlier reports, we here show how the quantitative analysis of time-resolved fluorescence can be used to obtain detailed information on the distribution of the pyrene-labelled A54145 (Py-A54145) between water and lipid membranes, as well as between different states of aggregation within the membrane. By performing this analysis at different calcium concentrations, we show that calcium-induced binding of monomeric Py-A54145 to the membrane is immediately followed by the formation of membrane-embedded oligomers. While this process is complete at 1 mM calcium, a well-defined second transition is observed when calcium is raised further. This second transition is apparent through increased excimer and reduced monomer fluorescence, respectively. It is consistent with an increase in the number of oligomer subunits, possibly arising from the alignment of two oligomers in opposite membrane leaflets [13].

Our study was carried out using the recently introduced Model-Free Analysis (MFA), which involves a global, simultaneous analysis of both monomer and excimer fluorescence decays [25, 26]. The successful dissection of the complex behaviour of A54145 illustrates that the MFA can be a powerful tool for the study of membrane-binding and/or oligomerizing peptides and proteins.

2. Material and Methods

2.1. Chemicals

The phospholipids 1,2-dimyristoyl-sn-glycero-3-phosphocholine (PC) and 1,2-dimyristoyl-sn-glycero-3-phospho-rac-(1'-glycerol) (PG) were purchased

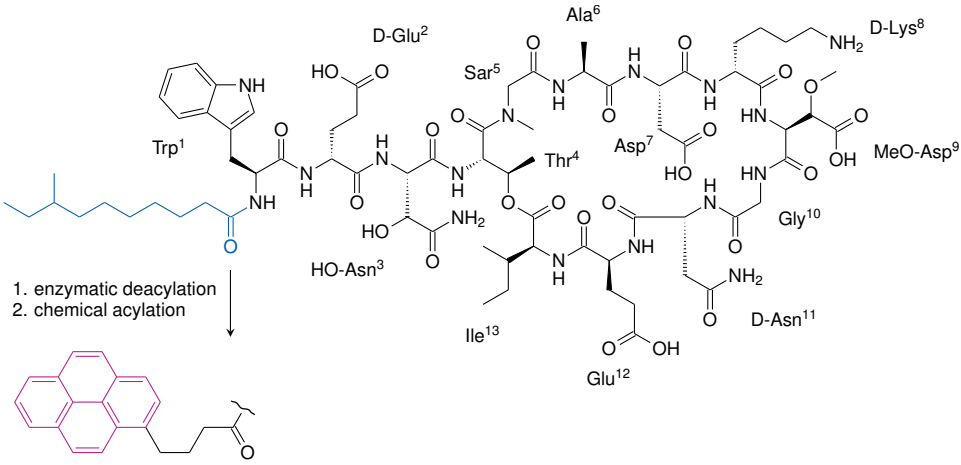

Figure 1: Structure of native A54145 Factor D [1] and of the pyrene-butanoyl label that was substituted for its native iso-decanoyl residue (blue) to produce Py-A54145. Non-standard acronyms: Sar, sarcosine; MeO-Asp, methoxy-aspartate; HO-Asn, hydroxy-asparagine. Details of the semisynthesis and purification of Py-A54145 are given in the Supporting Materials.

from Avanti Polar Lipids and used as received. A54145-Factor D (A54145) and polymer-supported *Actinoplanes utahensis* deacylase were gifts from Cubist Pharmaceuticals (Lexington, Massachusetts, USA). The structures of A54145 and Py-A54145 are illustrated in Figure 1; details of the Py-A54145 synthesis are given in Part A of the Supporting Materials.

2.2. Preparation of liposomes

PC and PG at equimolar ratio, or PC alone, were dissolved in a 3:1 mixture of chloroform:methanol. The solvent was evaporated under a stream of nitrogen in a round bottom flask, followed by evacuation for 3 hours. The lipid film was resuspended with HEPES buffer (20 mM HEPES/NaOH, 150 mM NaCl, pH 7.4), and the suspension was extruded 10-15 times through 100 nm polycarbonate membranes using a nitrogen-pressurized device [27]. The total lipid concentration for the fluorescence measurements was 250 μM and the liposome solutions were kept at 30°C.

2.3. Antibacterial activity of A54145 and Py-A54145

A54145 and Py-A54145 were serially diluted in LB broth supplemented with 5 mM $CaCl_2$. Each serial dilution was inoculated with 1% (v/v) of an overnight culture of *Bacillus subtilis* ATCC 1046, and the culture tubes were incubated at 37°C overnight with shaking. The growth was evaluated visually. The MIC

(minimum inhibitory concentration) was taken to be the lowest concentration without any visible turbidity.

2.4. Fluorescence measurements

All fluorescence experiments were carried out at 30°C with Py-A54145 (2 μM, unless stated otherwise) in buffer or in liposome suspensions, containing either 125 μM each of PC and PG or 250 μM of PC only. The samples were not deaerated. Samples were incubated for ≥5 minutes at the same temperature before the measurements were begun.

Steady-state fluorescence spectra were acquired on a Photon Technology International LS-100 spectrofluorimeter equipped with a continuous Ushio UXL-75Xe Xenon arc lamp and a PTI 814 photomultiplier detection system. The excitation wavelength was set at 344 nm and the fluorescence spectra were acquired from 350 to 600 nm. The monomer fluorescence intensity (I_M) was determined by taking the integral under the fluorescence spectrum between 372 and 378 nm. Similarly, integration of the fluorescence signal between 500 and 530 nm yielded the fluorescence intensity of the excimer (I_E).

Time-resolved fluorescence decays were obtained (using the time-correlated single photon counting technique) on an IBH Ltd. time-resolved fluorimeter equipped with an IBH 340 nm NanoLED as well as excitation and emission monochromators. The Py-A54145 solutions were excited at 344 nm and the fluorescence decays of the pyrene monomer and excimer were acquired at 375 and 510 nm, respectively. On the emission side, the instrument was additionally fitted with 370 and 495 nm cut-on filters, respectively, in order to prevent residual stray light scattered by the liposome suspension from reaching the detector. The fluorescence decays were acquired over 1,024 channels with 40,000 and 20,000 counts at the decay maximum for the pyrene monomer in buffer and the pyrene excimer in PC/PG membranes or 40,000 counts at the decay maximum of the pyrene monomer in PC or PC/PG membranes.

2.5. Analysis of the fluorescence decays

The fluorescence decays were analysed separately with sums of exponentials or globally with the Model-Free Analysis [25, 26]. The pre-exponential factors and decay times were optimized using the Marquardt-Levenberg algorithm [28]. The fits were considered satisfactory when the χ^2 was smaller than 1.3 and the weighted residuals and autocorrelation of the residuals were randomly distributed around zero. A detailed description of these analyses is provided in the Supporting Materials. All parameters retrieved from the analysis of the fluorescence decays are listed in Tables S1-S8 of the Supporting Materials.

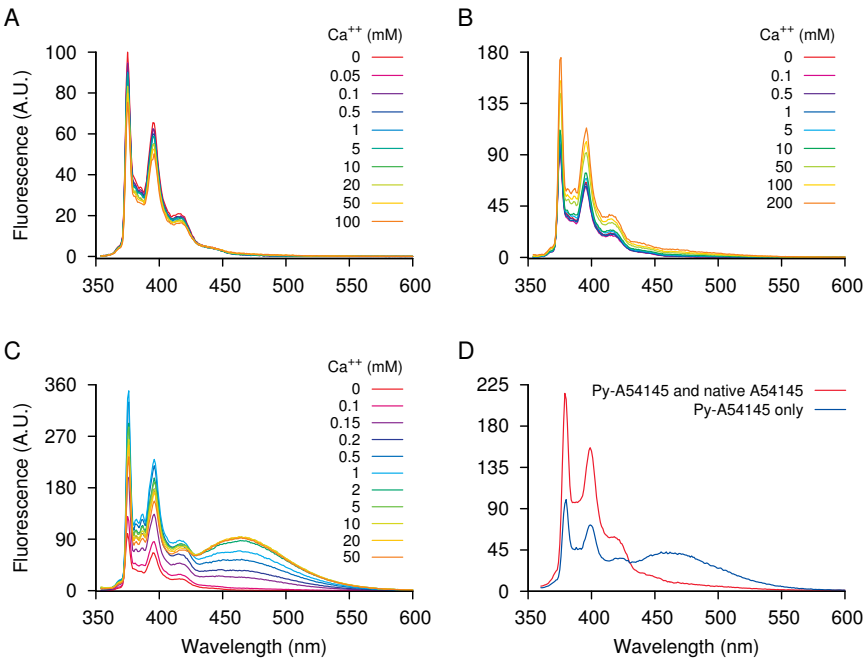

Figure 2: Fluorescence spectra of 2 μM Py-A54145 in the presence of Ca^{2+} incubated with buffer (A), PC liposomes (B), or PG/PC liposomes (C,D). In A–C, the intensity observed without Ca^{2+} at 375 nm was arbitrarily set to 100, and all other fluorescence spectra were scaled accordingly. In D, 0.5 μM Py-A54145 was incubated, with or without a fivefold excess of unlabelled native A54145, with PC/PG membranes and 5 mM Ca^{2+}. The peak intensity of the pure Py-A54145 sample was set to 100. The excitation wavelength was 344 nm throughout.

3. Results

3.1. Antibacterial activity of Py-A54145

The MIC of both native A54145 and Py-A54145 against *Bacillus subtilis* was 0.75 μg/ml, indicating that Py-A54145 retains full activity and is a valid model to study the activity of A54145. The observation agrees with previous observations on daptomycin, which also tolerates substitutions of its native fatty acyl residue with other hydrophobic moieties [15, 29].

3.2. Phosphatidylglycerol facilitates A54145 membrane binding and oligomerization

Figure 2 shows the effects of calcium on the steady-state fluorescence spectrum of Py-A54145 without liposomes and with PC or PC/PG liposomes, respectively. All spectra exhibit a series of sharp peaks between 370 and 420 nm, which

are typical of the pyrene monomer. With PC/PG liposomes, a broad, structureless emission band centred at 480 nm is also apparent that is characteristic of the pyrene excimer.

In the absence of liposomes, the fluorescence intensity of the pyrene monomer decreased by approximately 20% when the Ca^{2+} concentration was increased from 0 to 100 mM. This observation suggests that calcium binds to A54145 in solution, which has previously been documented with daptomycin [30]. The absence of excimer emission indicates that Py-A54145 does not aggregate in solution at low micromolar concentrations, which agrees with prior observations on daptomycin using FRET [8].

In the presence of PC liposomes, the intensity of the Py-A54145 monomer increases rather than decreases upon addition of calcium. The increase in monomer intensity suggests that pyrene enters a more hydrophobic environment, which is consistent with binding of Py-A54145 monomers to the membrane. The fluorescence intensity at 480 nm is somewhat higher than in buffer, indicating some measure of excimer formation. This would be expected from the concentrating effect of membrane binding, which would promote diffusional encounters between excited and ground state pyrene monomers. However, excimer fluorescence remains very low relative to monomer fluorescence.

With PC/PG liposomes, the monomer intensity increases much more readily and at much lower Ca^{2+} concentrations than is observed with PC membranes. A strong excimer signal emerges concomitantly, which indicates much closer interaction between the Py-A54145 molecules. A straightforward explanation for the strong excimer signal is that Py-A54145 undergoes oligomerization. Within an oligomer, the distances for diffusional encounters between pyrene labels are much smaller than those between molecules diffusing independently in the membrane, and therefore the likelihood of excimer formation increases.

The assumed correlation of excimer formation and A54145 oligomerization is further supported by the finding that the excimer fluorescence of a fixed amount of Py-A54145 can be suppressed by the addition of unlabelled A54145. If excimers arose from collisional encounters of membrane-bound monomers only, their formation should depend solely on the concentration of membrane-bound Py-A54145 and be unaffected by the presence or absence of unlabelled A54145. On the other hand, if the labelled and unlabelled species form hybrid oligomers, many of the Py-A54145 molecules contained in these hybrids should be surrounded by unlabelled neighbours and thus be unable to form excimers. Monomer fluorescence should be increased, and excimer fluorescence diminished, as is indeed observed (see Figure 2D).

The behaviour of Py-A54145 described thus far is consistent with results reported previously for daptomycin using perylene excimer fluorescence [15].

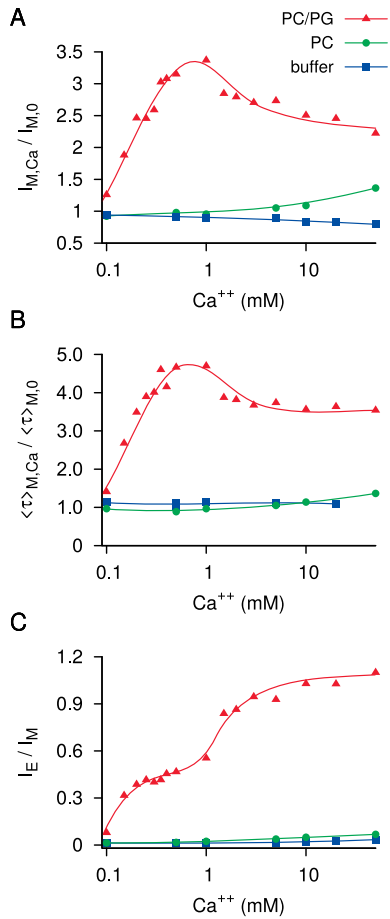

Figure 3: Calcium effects on the steady-state intensity (A) and the fluorescence lifetime (B) of Py-A54145 monomers, and on the ratio of steady-state excimer to monomer emission (C). The y axes in A and B show the monomer intensity and lifetime, respectively, at a given Ca^{2+} concentration relative to that obtained without Ca^{2+}. Monomer and excimer intensities were taken at 375 and 480 nm, respectively. Lifetimes in B are weighted averages obtained from three-exponential fit (see Supplementary Materials). Lines are visual aids without physical meaning.

However, a novel observation is that, on PC/PG membranes, the response of Py-A54145 to increasing Ca^{2+} levels occurs in two distinct phases. This biphasic response is seen in Figure 2C and, more clearly, in Figure 3. Panel A of the latter figure shows the steady-state intensity of the pyrene monomer as a function of Ca^{2+}, while panel B shows the number-average monomer lifetime, which was obtained by fitting individual monomer decays with sums of exponentials (see Equation S1 and Tables S1-S4 in the Supporting Materials). Both rise rapidly to-

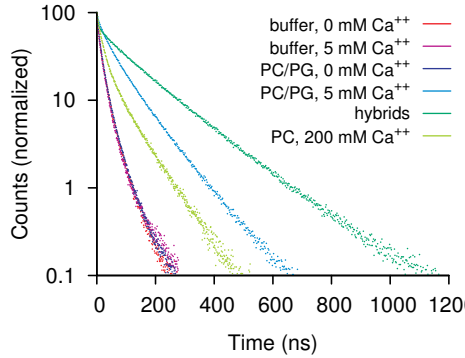

Figure 4: Time-resolved monomer fluorescence decays for Py-A54145 (2 μM) under different conditions. The sample labelled "hybrids" was incubated with PC/PG membranes and Ca^{2+} but additionally contained a ninefold molar excess of unlabelled A54145. Lifetime parameters for the various decays are listed in the Supporting Materials (Tables S1-S3 and S8).

ward a maximum at 0.5–1 mM Ca^{2+}. Increasing the Ca^{2+} concentration beyond this point causes them to drop back again. In contrast, the excimer intensity, which is shown relative to the monomer intensity in panel C, exhibits another steep rise and approaches a plateau a approximately 10 mM Ca^{2+}.

We also note that, in buffer or with PC membranes, all changes to any of the parameters are minor and occur only at higher Ca^{2+} concentrations. These observations corroborate the dominant role of PG in the membrane interaction of Py-A54145.

Time-resolved pyrene monomer fluorescence (Figures 3B and 4) agrees with the steady-state experiments. The decay time is longer with PC/PG membranes than with Py-A54145 in buffer or on PC membranes, and it is yet longer for hybrid oligomers of Py-A54145 and unlabelled A54145. These findings reinforce the notion that A54145 interacts differently with PC and PC/PG membranes.

3.3. Quantitative analysis of time-resolved monomer and excimer fluorescence

The second calcium-dependent transition that is observed on PC/PG membranes raises the question how exactly the two states of A54145 before and after this transition differ from one another. To address it, we applied an analytical method that we have described previously [25, 26], and which we refer to as the *Model-Free Analysis*.

3.3.1. Assumptions

In order to adapt the Model-Free Analysis to the A54145/membrane system, we made the following assumptions, which are illustrated in Figure 5:

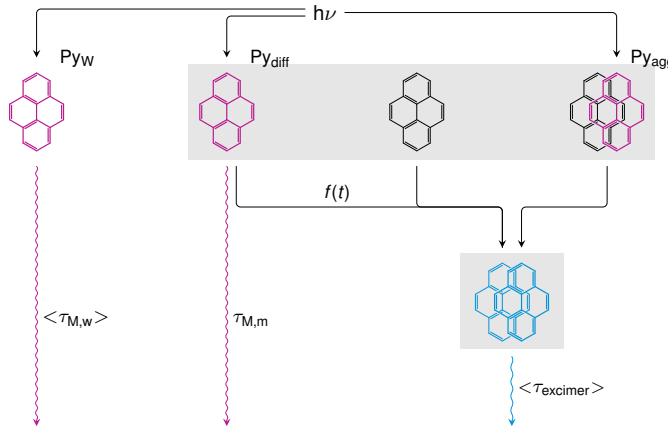

Figure 5: Assumed fluorescent states and transitions of Py-A54145 in the presence of PC/PG membranes. A54145 molecules that reside in water do not aggregate, and accordingly the attached pyrene moieties (Py_W) emit only monomer fluorescence. In the membrane, excited pyrene moieties can form excimers by diffusion (Py_{diff}); the rate of this process is governed by the function $f(t)$. Membrane-bound pyrene moieties can also form dimeric aggregates before excitation (Py_{agg}), which will contribute to excimer fluorescence only. Angular brackets signify the use of multiple lifetime components for the state in question.

1. Py-A54145 can reside in water or in the lipid bilayer.
2. Pyrene moieties that reside in water exhibit only monomer fluorescence. This is supported by the data shown in Figure 2A.
3. Pyrene moieties of membrane-bound Py-A54145 can emit excimer fluorescence or monomer fluorescence. Excimers can form through diffusional encounters between excited and ground-state monomers, or alternatively from aggregates of two ground-state molecules.
4. Dissociation of excimers to excited-state monomers is neglected. This assumption is reasonable for temperatures below 35°C [25, 31].

The existence of ground-state pyrene aggregates (Py_{agg} in Figure 5) in the PC/PG membrane can be demonstrated by fitting the time-resolved excimer emission with a sum of exponentials. In such a fit, diffusional excimer formation (Py_{diff}) will be captured by negative pre-exponential factors, whereas excimer decay will give rise to positive pre-exponential factors. If excimers formed by diffusion only, the sums of negative and positive pre-exponential factors should match [32, 33]. However, the negative pre-exponential factors amount to only -73 ± 4% of the positive ones (see Supporting Materials, Table S4); the difference must arise from direct excitation of ground-state pyrene aggregates.

Since our analysis is based on a set of assumptions, one might ask exactly what is meant by referring to it as *model-free*. The term denotes the approach to analysing the rate of diffusional excimer formation, which is named $f(t)$ in Figure 5. The conventional approach is to first formulate a physical model that predicts $f(t)$ from assumptions about the spatial distribution and motional freedom of pyrene monomers (see for example references 31, 34–36), and then to obtain the parameters of the chosen model by numerically fitting it to measured fluorescence decays. In contrast, the Model-Free Analysis does not assume a specific physical model; instead, it simply approximates $f(t)$ numerically with an appropriate number of exponential terms. Physical interpretations of the parameters obtained in this manner are only considered after the fact.

The advantage of this agnostic approach is that it is simple enough to allow for a simultaneous global analysis of monomer and excimer decays. From the scheme in Figure 5, it is clear that the exponential terms that represent $f(t)$ must be present—with opposite signs, since excimers are gained as monomers are lost—in the decays of both the monomer and the excimer. The Model-Free Analysis enforces this constraint while simultaneously fitting both decays, which reduces the statistical indeterminacy of the final result.

3.3.2. Experimental constraints

As depicted in Figure 5, we assume multiple populations of peptide-bound pyrene, which moreover may decay with multiple lifetimes. This results in a rather large number of variable parameters overall. In order to make the analysis more stringent, some of these parameters must therefore be constrained experimentally. This was done as follows:

1. The fluorescence decay of pyrene moieties in water (Py_W) was measured on a sample of Py-A54145 in buffer, in the absence of any liposomes. This decay was fitted with three exponential terms. The lifetimes and their associated pre-exponential factors thus obtained were treated as a single linear component when fitting all other monomer decays in the Model-Free Analysis; that is, the contribution of Py_W was represented in the global fit by only a single free parameter.
2. The lifetime of the membrane-bound pyrene monomer (denoted as $\tau_{M,m}$ in Figure 5) was determined on a sample of Py-A54145 with a ninefold excess of unlabelled A54145 that was incubated with PC/PG membranes (cf. Figure 4). In the hybrid oligomers that will form under these conditions, most Py-A54145 molecules will be surrounded by unlabelled A54145 neighbours, and the pyrene moieties will thus be unable to form excimers.

Therefore, the monomer decay of such a sample should be dominated by $\tau_{M,m}$.
In a three-exponential fit of the monomer decay, a lifetime of 170 ns accounted for 55% of the total pre-exponential weight (see Table S8 in Supporting Materials). This lifetime was used as the value of $\tau_{M,m}$ of all samples in the Model-Free Analysis.

3. The time course of excimer fluorescence is fairly complex, as excimers both form and decay on similar time scales. In order to constrain the rate of excimer formation (named $f(t)$ in Figure 5), monomer and excimer decays were acquired on a sample of Py-A54145 that was incubated with PC/PG liposomes and high Ca^{2+} (20 mM). Under these conditions, Py_W was taken as negligible, so that the monomer decay will solely be defined by the previously determined $\tau_{M,m}$ and $f(t)$.
Monomer and excimer decay curves were fitted globally according to Equations S9 and S10. In these fits, $f(t)$ was represented by three variable exponential terms, which were imposed on both monomer decay and excimer formation. The fit also allowed for two variable exponential terms for excimer decay. The lifetimes obtained for the two excimer decay terms were then fixed in all other Model-Free Analysis runs.

After applying these constraints, the global fit retains 10 freely variable parameters (see page 19 in the Supporting Materials); this is comparable to fitting a single decay using 5 parameters. Figure 6 shows an example of a Model-Free Analysis fit carried out in this manner. The decays of both the monomer and the excimer are fitted well, with small and evenly distributed residuals and autocorrelations. The excimer time course exhibits a clear initial rise, which represents the formation of excimers through diffusional encounters of monomers.

3.3.3. Resulting parameters

The key parameters retrieved by the Model-Free Analysis include the molar fractions of the various states of fluorescent pyrene moieties (cf. Figure 5), as well as the average rate constant of diffusional excimer formation ($<k>$). Note that $<k>$ is not a conventional bimolecular rate constant; instead, it is a pseudo-unimolecular parameter that measures how readily a given excited monomer will find a ground-state molecule to form an excimer (see Equations S6 and S7 in the Supporting Materials for its definition and its relation to $f(t)$, respectively). A change in $<k>$ usually reflects a structural change to the pyrene-labelled macromolecule that affects the mobility or local concentration of monomeric pyrene residues. In contrast, a change in the molar fractions usually indicates a change in the solubility or binding of the labelled molecules [33, 37].

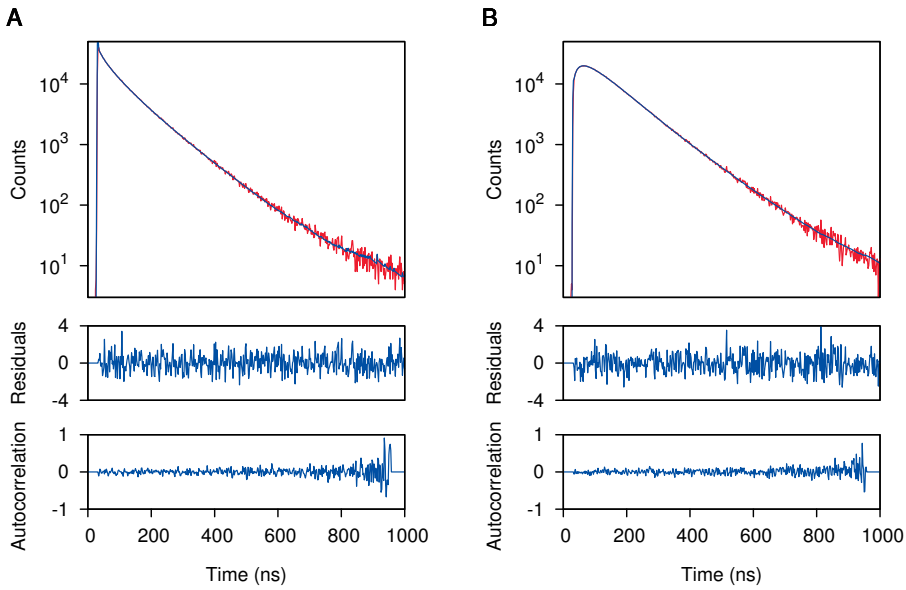

Figure 6: Model-Free Analysis: Example of a global fit of time-resolved fluorescence of pyrene monomers (A; λ_{ex}: 344 nm, λ_{em}: 375 nm) and excimers (B; λ_{ex}: 344 nm, λ_{em}: 510 nm). Experimental conditions: Py-A54145 in PC/PG liposome suspension with 5 mM Ca^{2+}. The overall χ^2 of the global fit is 1.06.

A fuller explanation of the Model-Free Analysis, which is given in Parts C and D of the Supporting Materials, details how the above parameters are obtained from the global fits, while Part E addresses the experimental error associated with the retrieved parameters and show that the analysis is reliable. Figure 7 shows how these parameters vary with the Ca^{2+} concentration. The unbound fraction (Py_W) drops rapidly to near zero with increasing Ca^{2+} (Figure 7A); this agrees with the observations from steady-state fluorescence (cf. Figure 3).

Figure 7B shows the relative abundance of membrane-associated pyrene molecules that form excimers by diffusion (Py_{diff}) or by aggregation (Py_{agg}). Py_{diff} dominates at all calcium concentrations; this resembles previous findings with pyrene-labelled polymers in organic solvents [38], as well as with micelles of pyrene-labeled gemini surfactants [33], and it suggests that pyrene resides inside a locally disordered environment within the apolar core of the membrane. Nevertheless, Py_{agg} appears to undergo a small step increase at a Ca^{2+} concentration slightly above 1 mM. At virtually the same Ca^{2+} level, we observe a doubling in the average rate of diffusional excimer formation ($<k>$).

In the steady-state experiments, we had noticed that the excimer fluorescence underwent a pronounced increase just above 1 mM Ca^{2+} (cf. Figure 3),

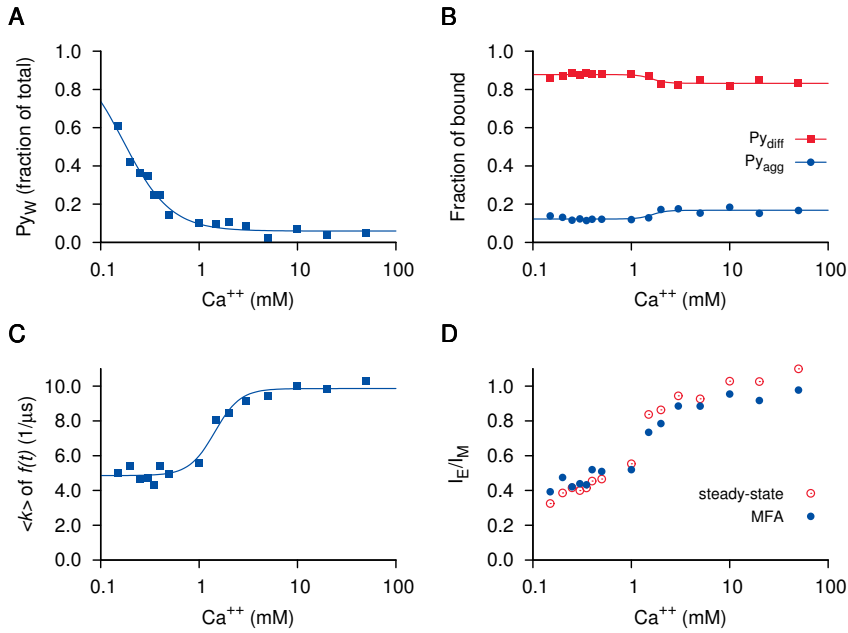

Figure 7: Parameters retrieved from the Model-Free Analysis, as functions of the Ca^{2+} concentration (cf. Figure 5 for acronyms). A: molar fraction of Py_W. B: Py_{diff} and Py_{agg}, as fractions of the overall membrane-bound pyrene moieties. C: average rate constant of diffusional excimer formation, calculated according to Equation S6. Lines represent fits to the Hill equation; the fitted parameters are listed in Part H of the Supporting Materials. D: ratio of excimer to monomer emission as reconstructed from the Model-Free Analysis (MFA), overlaid to the steady-state results (cf. Figure 3C).

and the same is also seen when the ratio of excimer to monomer fluorescence is reconstructed using the parameters retrieved from the Model-Free Analysis (Figure 7D; details in Part D of the Supporting Materials). From the latter, we now see that this increase does not involve a major change in Py_{diff} or Py_{agg}; instead, it is almost entirely caused by an increase in the rate of diffusional excimer formation within the Py_{diff} population.

4. Discussion

In order to make sense of the collective findings, we must first distinguish between the oligomerization—that is, peptide-peptide interaction—of A54145 on the one hand, and the diffusional association or aggregation of pyrene moieties attached to the A54145 molecules on the other. Pyrene monomer and excimer fluorescence may arise from both monomeric and oligomeric Py-A54145. However, as noted in section 3.2, both in water and when bound to PC membranes,

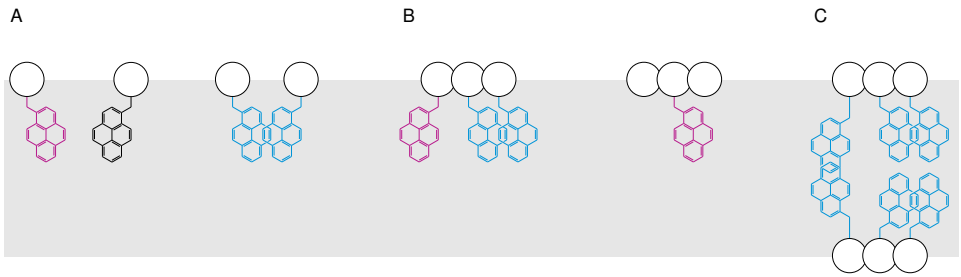

Figure 8: Proposed interpretation of pyrene fluorescence in terms of A54145 function. A: Membrane-bound Py-A54145 monomers may form excimers by diffusion. This process will be concentration-dependent and inefficient; it likely occurs on PC membranes. B: On PC/PG membranes, binding of the first Ca^{2+} ion to Py-A54145 causes formation of small oligomers, which increases excimer fluorescence. Excimer fluorescence is suppressed by mixing Py-A54145 with an excess of unlabelled A54145. C: Binding of the second Ca^{2+} ion increases the oligomer size, possibly by aligning two small oligomers across both membrane leaflets. This further increases the efficiency of excimer formation.

Py-A54145 exhibits very little excimer fluorescence. Like daptomycin [8, 15], A54145 most likely binds to PC membranes as a monomer. While membrane binding will greatly concentrate the monomeric Py-A54145, the highly viscous membrane environment will counteract the formation of excimers by diffusion. Therefore, efficient excimer formation can only be expected after Py-A54145 has formed oligomers.

The rate of diffusional encounters between membrane-bound Py-A54145 monomers will vary with their concentration. In contrast, after oligomerization, excimers will form mostly between neighbouring subunits of the same oligomer, and the total concentration of membrane-bound Py-A54145 should have little or no effect on the likelihood of excimer formation. With this in mind, we can examine what the pyrene fluorescence tells us about the behaviour of A54145 on PC/PG membranes (cf. Figure 8).

4.1. Binding of Py-A54145 to PC/PG membranes

The increase of monomer intensity and lifetime, the decrease in Py_W, and the high fractional contribution of Py_{diff} to the excimer intensity all indicate that Py-A54145 binds progressively at low Ca^{2+} concentration. The rate of the drop of Py_W with increasing Ca^{2+} (Figure 7A) suggests some measure of cooperativity (see Table S9 in Part G of the Supporting Materials), which would agree with the association of two Ca^{2+} ions to each lipopeptide molecule [14], as well as with the oligomerization of the membrane-bound Py-A54145. However, due to some degree of static quenching, Py_W may slightly underestimate the fraction of unbound Py-A54145. This complicates an accurate analysis of binding, which

may be more amenable to calorimetric methods. On the other hand, fluorescence is more suitable for dissecting the behaviour of the bound lipopeptide, which was the main focus of this study.

4.2. A54145 oligomerizes concomitantly with membrane binding

From the lack of excimer fluorescence of Py-A54145 in solution (cf. Figure 2A), it is clear that A54145 does not oligomerize prior to membrane binding, at least not at the low yet biologically relevant lipopeptide concentrations employed here. This confirms previous studies on the related lipopeptide daptomycin [8, 39]. The question is, then, how tightly membrane binding of A54145 is coupled to the formation of oligomers.

Between 0.1 and 1 mM Ca^{2+}, the contribution from Py_W to the overall pyrene monomer fluorescence decreases from about 75% to approximately 5% (cf. Figure 7A), which implies a strong increase in membrane-bound Py-A54145. If the bound lipopeptide stayed monomeric, the pseudo-unimolecular rate constant of excimer formation by diffusion ($<k>$) should increase in proportion to its concentration in the membrane; however, this rate constant remains virtually unchanged (cf. Figure 7C). This finding indicates that the membrane-associated Py-A54145 is already oligomeric at this stage. In keeping with this interpretation, excimer formation on PC/PG membranes far exceeds that observed on pure PC membranes, to which daptomycin binds as a monomer [8]; this applies at all Ca^{2+} concentrations (cf. Figures 2 and 3). Pyrene monomer lifetimes are higher on PC/PG membranes than on PC membranes (see Tables S2 and S3 in Part F of Supporting Materials). This effect, as well as lateral phase segregation on PC/PG membranes [40], should cause a somewhat higher rate of excimer formation even between monomeric Py-A54145 molecules; nevertheless, the very high excimer intensity on PC/PG membranes strongly suggests oligomer formation.

4.3. Aggregation of fatty acyl residues precedes that of peptide moieties

We recently reported that the membrane interaction of daptomycin and A54145 occurs in two separate steps, each of which is driven by the binding of one Ca^{2+} ion [14]. Those experiments were carried out with the fluorescent dye acrylodan, which was attached to amino acid residues 6 and 8 in daptomycin and A54145, respectively. In the first step, acrylodan emission increased in intensity and blue-shifted, compatible with membrane binding. In the second step, acrylodan underwent self-quenching, indicating oligomerization.

The Ca^{2+} concentrations that will induce each of the two changes in acrylodan emission align very closely with those that were found here to induce the two stepwise increases in pyrene excimer formation. We therefore assume that

pyrene and acrylodan report on the same structural changes to the lipopeptide. It is notable, then, that pyrene excimer fluorescence detects oligomerization after binding of the first Ca^{2+} ion, while acrylodan self-quenching detects it only after binding of the second one.

The pyrene moiety in Py-A54145 is part of the fatty acyl tail of the molecule (see Figure 1), whereas acrylodan was attached to the peptide moieties. It therefore appears that the fatty acyl tails associate before the peptide moieties do, and that the initial oligomer must undergo a significant structural transition concomitantly with binding of the second calcium ion.

4.4. The second calcium-dependent transition may double the size of the oligomer

With Py-A54145, the second transition manifests itself by a doubling of the rate of diffusional excimer formation (cf. Figure 7C). Most likely, after the transition, each excited pyrene monomer now has a greater number of ground-state neighbours to engage with. The doubling of the rate can of course not strictly prove a doubling of the oligomer size; a conformational change that would bring the pyrenyl moieties into greater proximity within the oligomer is another possible explanation. Nevertheless, the observation does resonate with the previous proposal [13] that daptomycin oligomers may contain either four or eight subunits, depending on whether they span only one or both membrane leaflets. It appears possible, therefore, that the second Ca^{2+}-dependent transition reported by Py-A54145 corresponds to the alignment of two tetramers across both membrane leaflets, resulting in an octamer that presumably forms the functional transmembrane pore. This possibility needs to be addressed in future experiments.

At this point, one might wonder if the intermediate, presumably singly calcium-saturated state of daptomycin or A54145 has any functional significance in vivo. In the human body, the extracellular level of free calcium is approximately 1.25 mM, which suffices to drive daptomycin to the final, presumably doubly saturated state [14]. Similarly, in soil, which is the natural habitat of the daptomycin and A54145 producer organisms, calcium concentrations appear to be in the low millimolar range [41]. Therefore, while the calcium concentration required for complete saturation may differ depending on the lipid composition of the bacterial target membrane, there is no clear scenario to explicitly suggest that the singly saturated form is functionally important in vivo.

4.5. Limitations and approximations inherent in the Model-Free Analysis

While the conclusions reached here by the application of the Model-Free Analysis hopefully speak to the usefulness of this method, one should be aware

of its limitations. One is inherent in the relinquishment of a physical model for the excimer formation function $f(t)$. As illustrated here, the Model-Free Analysis subsumes the rate of excimer formation in a single parameter ($<k>$), which may entail the loss of some subtle information that a suitable physical model might have recovered. On the other hand, as is illustrated in the Supporting Materials (Figure S7, Part E), the value of $<k>$ is more robust than that of the individual lifetime components on which it is based. Accordingly, a physical model that assigns meaning to multiple separate lifetimes may be subject to greater experimental uncertainty.

In the current study, the excimer fluorescence was represented by two separate lifetime components. This approach is well supported by studies on model compounds that contain two pyrene residues linked by short organic spacer moieties. In such molecules, pyrene excimers may adopt two distinct conformations with different degrees of planar overlap and, accordingly, emission lifetimes [42, 43]. In the case of Py-A54145, there may well be more than two discrete excimer conformations. However, two lifetime components proved sufficient to accommodate the observed decays in the global fits. While the Model-Free Analysis is unable to determine the true number of excimer conformations and lifetimes, our interpretation of the results does not hinge on this question. Similar considerations apply to the chosen numbers of lifetimes for pyrene monomers in water and in the membrane.

4.6. Conclusion

In summary, this study provides novel insights into the action mode of Py-A54145, a model compound for the therapeutically important antibiotic daptomycin. It supports our previous hypothesis that A54145 interacts with membranes containing PG in two distinguishable Ca^{2+}-dependent steps [14], and it further indicates that an oligomeric state is reached already upon completion of the first step. More generally, our study demonstrates the usefulness of pyrene fluorescence to understand the behaviour of peptides that interact both mutually and with membranes, particularly when it is used in conjunction with the powerful Model-Free Analysis method.

Author contributions

TZ conducted all the experiments. ST synthesized Py-A54145. MP and ST developed the line of research revolving around the use of fluorescently labelled daptomycin analogues to determine how daptomycin interacts with lipid bilayers. MP suggested the use of time-resolved pyrene fluorescence to study the membrane interaction of A54145. JD analysed the fluorescence spectra and

decays, developed the version of the Model Free Analysis used to fit globally the monomer and excimer decays. JD and MP wrote the manuscript.

Acknowledgements

This work was supported by NSERC operating grants to JD (#201603-2013), MP (#250265-2013), and ST (#155283-2012).

Supporting material available

Synthesis of Py-A54145, detailed description of the Model-Free Analysis and its adaptation to fit the monomer and excimer decays of Py-A54145 in solution of PC/PG liposomes in the presence of Ca^{2+}. Error analysis of the parameters retrieved from the analysis of the fluorescence decays. Procedure applied to determine the natural lifetime of the pyrene label of Py-A54145 in PC/PG liposomes. Parameters retrieved from the fit of the fluorescence decays with sums of exponentials or according to the Model-Free Analysis. Parameters retrieved from the fits of the trends shown in Figure 7A-C with the Hill equation.

5. Bibliography

[1] Fukuda, D. S., M. Debono, R. M. Molloy, and J. S. Mynderse, 1990. A54145, a new lipopeptide antibiotic complex: microbial and chemical modification. *J Antibiot (Tokyo)* 43:601–606. http://view.ncbi.nlm.nih.gov/pubmed/2380108.

[2] Kosmidis, C., and D. P. Levine, 2010. Daptomycin: pharmacology and clinical use. *Expert Opin Pharmacother* 11:615–625. http://view.ncbi.nlm.nih.gov/pubmed/20163272.

[3] Alborn, W. E. J., N. E. Allen, and D. A. Preston, 1991. Daptomycin disrupts membrane potential in growing *Staphylococcus aureus*. *Antimicrob Agents Chemother* 35:2282–2287. http://www.ncbi.nlm.nih.gov/pubmed/1666494.

[4] Mascio, C., K. Townsend, N. Cotroneo, and J. Silverman, 2009. Microbiological Characterization of a Novel Lipopeptide Antibiotic with Activity in Pulmonary Surfactant. 49th Interscience Conference on Antimicrobial Agents and Chemotherapy, September 12–15, 2009, San Francisco, CA, American Society For Microbiology, Washington, DC.

[5] Zhang, T., J. K. Muraih, E. Mintzer, N. Tishbi, C. Desert, J. Silverman, S. Taylor, and M. Palmer, 2013. Mutual inhibition through hybrid oligomer formation of daptomycin and the semisynthetic lipopeptide antibiotic CB-182,462. *Biochim Biophys Acta* 1828:302–308. http://view.ncbi.nlm.nih.gov/pubmed/23084999.

[6] Silverman, J. A., L. I. Mortin, A. D. G. Vanpraagh, T. Li, and J. Alder, 2005. Inhibition of daptomycin by pulmonary surfactant: in vitro modeling and clinical impact. *J Infect Dis* 191:2149–2152. http://view.ncbi.nlm.nih.gov/pubmed/15898002.

[7] Nguyen, K. T., X. He, D. C. Alexander, C. Li, J.-Q. Gu, C. Mascio, A. V. Praagh, L. Mortin, M. Chu, J. A. Silverman, P. Brian, and R. H. Baltz, 2010. Genetically Engineered Lipopeptide Antibiotics Related to A54145 and Daptomycin with Improved Properties. *Antimicrob Agents Chemother* 54:1404–1413. http://www.ncbi.nlm.nih.gov/pubmed/20086142.

[8] Muraih, J. K., A. Pearson, J. Silverman, and M. Palmer, 2011. Oligomerization of daptomycin on membranes. *Biochim Biophys Acta* 1808:1154–1160. http://view.ncbi.nlm.nih.gov/pubmed/21223947.

[9] Zhang, T., J. Muraih, B. MacCormick, J. Silverman, and M. Palmer, 2014. Daptomycin forms cation- and size-selective pores in model membranes. *Biochim Biophys Acta* 1838:2425–2430. http://www.ncbi.nlm.nih.gov/pubmed/24857935.

[10] Baltz, R. H., 2009. Daptomycin: mechanisms of action and resistance, and biosynthetic engineering. *Curr Opin Chem Biol* 13:144–151. http://www.ncbi.nlm.nih.gov/pubmed/19303806.

[11] Davlieva, M., W. Zhang, C. A. Arias, and Y. Shamoo, 2013. Biochemical characterization of cardiolipin synthase mutations associated with daptomycin resistance in enterococci. *Antimicrob Agents Chemother* 57:289–296. http://view.ncbi.nlm.nih.gov/pubmed/23114777.

[12] Mishra, N. N., S.-J. Yang, L. Chen, C. Muller, A. Saleh-Mghir, S. Kuhn, A. Peschel, M. R. Yeaman, C. C. Nast, B. N. Kreiswirth, A.-C. Crémieux, and A. S. Bayer, 2013. Emergence of daptomycin resistance in daptomycin-naïve rabbits with methicillin-resistant Staphylococcus aureus prosthetic joint infection is associated with resistance to host defense cationic peptides and mprF polymorphisms. *PLoS One* 8:e71151. http://view.ncbi.nlm.nih.gov/pubmed/23990934.

[13] Zhang, T., J. K. Muraih, N. Tishbi, J. Herskowitz, R. L. Victor, J. Silverman, S. Uwumarenogie, S. D. Taylor, M. Palmer, and E. Mintzer, 2014. Cardiolipin prevents membrane translocation and permeabilization by daptomycin. *J Biol Chem* 289:11584–11591. http://view.ncbi.nlm.nih.gov/pubmed/24616102.

[14] Taylor, R. M., K. Butt, B. Scott, J. K. Muraih, T. Zhang, S. D. Taylor, M. Palmer, and E. M. Mintzer, 2016. Two successive calcium-dependent transitions mediate membrane binding and oligomerization of daptomycin and the related antibiotic A54145. *BBA Biomembranes* 1858:1999–2005.

[15] Muraih, J. K., J. Harris, S. D. Taylor, and M. Palmer, 2012. Characterization of daptomycin oligomerization with perylene excimer fluorescence: stoichiometric

binding of phosphatidylglycerol triggers oligomer formation. *Biochim Biophys Acta* 1818:673–678. http://view.ncbi.nlm.nih.gov/pubmed/22079564.

[16] Betcher-Lange, S. L., and S. S. Lehrer, 1978. Pyrene excimer fluorescence in rabbit skeletal alphaalphatropomyosin labeled with N-(1-pyrene)maleimide. A probe of sulfhydryl proximity and local chain separation. *J Biol Chem* 253:3757–3760. http://view.ncbi.nlm.nih.gov/pubmed/565773.

[17] Duhamel, J., M. A. Winnik, F. Baros, J. C. Andre, and J. M. G. Martinho, 1992. Transient effects on diffusion-controlled reactions. 11. Diffusion effects on pyrene excimer kinetics: determination of the excimer formation rate coefficient time dependence. *J. Phys. Chem* 96:9805–9810. http://dx.doi.org/10.1021/j100203a042.

[18] Kalyanasundaram, K., and J. K. Thomas, 1977. Environmental effects on vibronic band intensities in pyrene monomer fluorescence and their application in studies of micellar systems. *J. Am. Chem. Soc* 99:2039–2044. http://dx.doi.org/10.1021/ja00449a004.

[19] Dong, D. C., and M. A. Winnik, 1982. The Py scale of solvent polarities. solvent effects on the vibronic fine structure of pyrene fluorescence and empirical correlations with et and y values. *Photochem Photobiol* 35:17–21. http://dx.doi.org/10.1111/j.1751-1097.1982.tb03805.x.

[20] Dong, D. C., and M. A. Winnik, 1984. The Py scale of solvent polarities. *Can. J. Chem* 62:2560–2565. http://dx.doi.org/10.1139/v84-437.

[21] Ishii, Y., and S. S. Lehrer, 1991. Two-site attachment of troponin to pyrene-labeled tropomyosin. *J Biol Chem* 266:6894–6903. http://view.ncbi.nlm.nih.gov/pubmed/2016303.

[22] Tamamizu-Kato, S., M. G. Kosaraju, H. Kato, V. Raussens, J.-M. Ruysschaert, and V. Narayanaswami, 2006. Calcium-triggered membrane interaction of the alpha-synuclein acidic tail. *Biochemistry* 45:10947–10956. http://view.ncbi.nlm.nih.gov/pubmed/16953580.

[23] Kono, M., Y. Okumura, M. Tanaka, D. Nguyen, P. Dhanasekaran, S. Lund-Katz, M. C. Phillips, and H. Saito, 2008. Conformational flexibility of the N-terminal domain of apolipoprotein a-I bound to spherical lipid particles. *Biochemistry* 47:11340–11347. http://view.ncbi.nlm.nih.gov/pubmed/18831538.

[24] Mizuguchi, C., M. Hata, P. Dhanasekaran, M. Nickel, M. C. Phillips, S. Lund-Katz, and H. Saito, 2012. Fluorescence analysis of the lipid binding-induced conformational change of apolipoprotein E4. *Biochemistry* 51:5580–5588. http://view.ncbi.nlm.nih.gov/pubmed/22730894.

[25] Duhamel, J., 2012. New Insights in the Study of Pyrene Excimer Fluorescence to Characterize Macromolecules and their Supramolecular Assemblies in Solution. *Langmuir* 24:6527–6538. http://view.ncbi.nlm.nih.gov/pubmed/22423596.

[26] Duhamel, J., 2014. Global analysis of fluorescence decays to probe the internal dynamics of fluorescently labeled macromolecules. *Langmuir* 30:2307–2324. http://view.ncbi.nlm.nih.gov/pubmed/24175714.

[27] Mayer, L. D., M. J. Hope, and P. R. Cullis, 1986. Vesicles of variable sizes produced by a rapid extrusion procedure. *Biochim Biophys Acta* 858:161–168. http://www.ncbi.nlm.nih.gov/pubmed/3707960.

[28] Press, W. H., S. A. Teukolsky, W. T. Vetterling, and B. P. Flannery, 1992. Numerical Recipes: The art of scientific computing, volume 683. Cambridge Univ. Press.

[29] Debono, M., B. J. Abbott, R. M. Molloy, D. S. Fukuda, A. H. Hunt, V. M. Daupert, F. T. Counter, J. L. Ott, C. B. Carrell, and L. C. Howard, 1988. Enzymatic and chemical modifications of lipopeptide antibiotic A21978C: the synthesis and evaluation of daptomycin (LY146032). *J Antibiot (Tokyo)* 41:1093–1105. http://www.ncbi.nlm.nih.gov/pubmed/2844711.

[30] Jung, D., A. Rozek, M. Okon, and R. E. W. Hancock, 2004. Structural transitions as determinants of the action of the calcium-dependent antibiotic daptomycin. *Chem Biol* 11:949–957. http://www.ncbi.nlm.nih.gov/pubmed/15271353.

[31] Martins, J., and E. Melo, 2001. Molecular mechanism of lateral diffusion of py(10)-PC and free pyrene in fluid DMPC bilayers. *Biophys J* 80:832–840. http://view.ncbi.nlm.nih.gov/pubmed/11159450.

[32] Siu, H., and J. Duhamel, 2006. Associations between a pyrene-labeled hydrophobically modified alkali swellable emulsion copolymer and sodium dodecyl sulfate probed by fluorescence, surface tension, and viscometry. *Macromolecules* 39:1144–1155. http://dx.doi.org/10.1021/ma0519563.

[33] Keyes-Baig, C., J. Duhamel, and S. Wettig, 2011. Characterization of the behavior of a pyrene substituted gemini surfactant in water by fluorescence. *Langmuir* 27:3361–3371. http://view.ncbi.nlm.nih.gov/pubmed/21341800.

[34] Masanori, T., 1975. Application of a generating function to reaction kinetics in micelles. Kinetics of quenching of luminescent probes in micelles. *Chem Phys Lett* 33:289–292.

[35] Strukelj, M., J. M. G. Martinho, M. A. Winnik, and R. P. Quirk, 1991. Intermolecular excimer formation for pyrene-end-capped polystyrene: a model for the termination process in free-radical polymerization. *Macromolecules* 24:2488–2492. http://dx.doi.org/10.1021/ma00009a054.

[36] Duhamel, J., A. Yekta, M. A. Winnik, T. C. Jao, M. K. Mishra, and I. D. Rubin, 1993. A blob model to study polymer chain dynamics in solution. *J Phys Chem* 97:13708–13712. http://dx.doi.org/10.1021/j100153a046.

[37] Siu, H., and J. Duhamel, 2005. Comparison of the association level of a pyrene-labeled associative polymer obtained from an analysis based on two different models. *J Phys Chem B* 109:1770–1780. http://view.ncbi.nlm.nih.gov/pubmed/16851157.

[38] Kanagalingam, S., C. F. Ngan, and J. Duhamel, 2002. Effect of Solvent Quality on the Level of Association and Encounter Kinetics of Hydrophobic Pendants Covalently Attached onto a Water-Soluble Polymer. *Macromolecules* 35:8560–8570. http://dx.doi.org/10.1021/ma0207428.

[39] Qiu, J., and L. E. Kirsch, 2014. Evaluation of lipopeptide (daptomycin) aggregation using fluorescence, light scattering, and nuclear magnetic resonance spectroscopy. *J Pharm Sci* 103:853–861. http://view.ncbi.nlm.nih.gov/pubmed/24464772.

[40] Muraih, J. K., and M. Palmer, 2012. Estimation of the subunit stoichiometry of the membrane-associated daptomycin oligomer by FRET. *Biochim Biophys Acta* 1818:1642–1647. http://view.ncbi.nlm.nih.gov/pubmed/22387459.

[41] Suarez, D. L., J. D. Wood, and I. Ibrahim, 1992. Reevaluation of calcite supersaturation in soils. *Soil Sci Soc Am J* 56:1776–1784.

[42] Zachariasse, K. A., R. Busse, G. Duveneck, and W. Kühnle, 1985. Intramolecular monomer and excimer fluorescence with dipyrenylpropanes: double-exponential versus triple-exponential decays. *J Photochem* 28:237–253. http://www.sciencedirect.com/science/article/pii/0047267085870350.

[43] Fowler, M., V. Hisko, J. Henderson, R. Casier, L. Li, J. L. Thoma, and J. Duhamel, 2015. DiPyMe in SDS Micelles: Artifacts and Their Implications in the Interpretation of Micellar Properties. *Langmuir* 31:11971–11981. http://view.ncbi.nlm.nih.gov/pubmed/26465066.